Pergamon

Int. J. Heat Mass Transfer. Vol. 37, No. 5, pp. 727–736, 1994

0017–9310/94 $6.00+0.00

Theoretical study of combined conductive, convective and radiative heat transfer between plates and packed beds

J. D. LU,† G. FLAMANT and B. VARIOT

Institut de Science et de Génie des Matériaux et Procédés, CNRS, BP °5, Odeillo, 66125, Font-Romeu Cedex, France

(*Received* 7 *December* 1992 *and in final form* 7 *October* 1993)

Abstract—The forced convective heat transfer near a wall or a plate immersed in a packed bed at high temperature is considered in this paper. The non-Darcian effects are considered for the hydrodynamics and heat transfer and dependent scattering theory are taken into account for the radiation transfer. The discrete-ordinate method is used to solve the equation for radiation intensity. It is found from the numerical predictions that radiative heat transfer rate increases with a decrease of the convection–radiation parameter (Bo) or conduction–radiation parameter (N) and an increase of the Reynolds number. The effect of radiation on conduction–convection is determined by the sign of the net radiation absorbed by the particles. The radiation properties of the plate and the bed, as well as the direction of heat flux, have obvious influence on heat transfer in packed beds at high temperature.

INTRODUCTION

In recent years much attention has been paid to the non-Darcian phenomena in the case of boundary layer flow and heat transfer in porous media because of its importance in various applications, such as entrance regions in large tube reactors, external flows along buried pipes in packed beds, or flows adjacent to a single impermeable surface. For the cases of forced convection considered in this paper, Chandrasekhara and Vortmeyer [1] proposed a flow model for velocity distribution in a fixed porous bed under isothermal conditions, which considered the effects of boundary friction, inertial force and the variation of porosity along the radial direction. Vafai and Tien [2, 3] analyzed theoretically and experimentally the boundary and inertial effects on convective flow and heat and mass transfer for constant porosity media. An in-depth investigation of the channelling effect and its influence on heat transfer and flow through variable-porosity media was conducted by Vafai [4]. The effect of inter-pore mixing or dispersion on the forced heat transfer was studied by Plumb [5], Whitaker [6] and Cheng and Vortmeyer [7]. The complete influence of these non-Darcian effects to the forced convection near flat plates, in circular and in square columns is summarized by Tien and Hunt [8], Hunt and Tien [9], Tsotsas and Schlunder [10] and Chou *et al.* [11].

Unfortunately only few research works have been conducted on the problems of combined convection and radiation in packed beds [12], especially in the case of forced convection. Harris and Lenz [13] made an experimental study to measure the heat transfer through a packed bed contained between two horizontal concentric tubes with particle Reynolds numbers from zero to 90 and ratio of tube wall temperatures T_{out}/T_{in} from 1.5 to 3.2. The theoretical works previously published deal with natural convection in porous media contained in vertical cavities [14] and one dimensional forced fluid flow through a porous medium [15]. A theoretical model on combined transient conductive, convective and radiative heat transfer between vertical walls and fluidized beds was proposed recently by Flamant *et al.* [16]. So it seems necessary to make a detailed investigation for the combined convection and radiation in packed beds, since in some applications, such as fixed-bed catalytic reactors, packed-bed heat exchangers and metal processing, the radiation could be important when the operating temperature is high. The objective of this study is to present a theoretical analysis for the combined forced convection and radiation in packed beds along a flat plate. The interaction between different heat transfer modes is considered when the non-Darcian effects are included. The qualitative effects of controlling parameters on both convective and radiative components are also checked.

MATHEMATICAL DESCRIPTION

The heat exchanging element considered here is a flat plate with the length L and a constant temperature T_w (as shown in Fig. 1). The temperature of the packed bed far from the plate remains constant at T_B. For the mathematical analysis of the problem, the following assumptions are made.

† Present address: Department of Power Engineering, Huazhong University of Science and Technology, Wuhan, Hubei, 430074, P. R. of China.

NOMENCLATURE

a	absorption coefficient [m^{-1}]
B	constant in equation (9)
Bo	Boltzmann number, $(\rho C_p)_f u_\infty / \sigma T_h^3$
C	inertia coefficient [m^{-1}]
c	average interparticle distance [m]
C_p	specific thermal capacity [$J\,kg^{-1}\,K^{-1}$]
D, D^*	constant in equation (8)
d_p	particle diameter [m]
Da	Darcy number based on particle diameter, K_∞/d_p^2
I	nondimensional radiation intensity, $i/\sigma T_h^4$
i	radiation intensity [$W\,m^{-2}\,sr^{-1}$]
K	permeability [m^2]
k	conductivity [$W\,m^{-2}\,K^{-1}$]
N	Planck number, $K_{e\infty}^s \kappa_\infty / 4\sigma T_h^3$
Nu	Nusselt number based on particle diameter, $hd_p/k_{e\infty}^s$
Nu_x	local Nusselt number, $hx/k_{e\infty}^s$
P	scattering phase function
Pe	Peclet number based on particle diameter, $u_\infty d_p/\alpha_\infty^s$
Pe_x	local Peclet number, $u_\infty x/\alpha_\infty^s$
p	pressure [Pa]
q	heat flux density [$W\,m^{-2}$]
Re	Reynolds number based on particle diameter, ud_p/ν_f
Re_c	modified Reynolds number, $K_\infty C_\infty u_\infty/\nu_f$
T	temperature [K]
u	velocity [$m\,s^{-1}$]
w	weight of Gaussian quadrature
X	nondimensional longitudinal coordinate, x/d_p
x	longitudinal coordinate [m]
Y	nondimensional transverse coordinate, y/d_r
y	transverse coordinate [m].

Greek symbols

α	thermal diffusion coefficient [$m^2\,s^{-1}$]
β	parameter in equation (5)
γ	coefficient of dispersive conductivity
δ	porosity
ε	emissivity
θ	non-dimensional temperature, T/T_h
κ	extinction coefficient, $a+\sigma_s$
λ	wavelength of radiation
μ	$\cos\theta$
μ_f	dynamic viscosity [$kg\,m^{-1}\,s^{-1}$]
ν_f	kinetic viscosity [$m^2\,s^{-1}$]
ρ	density [$kg\,m^{-3}$]
σ	Stefan–Boltzmann constant [$W\,m^{-2}\,K^{-4}$]
σ_s	scattering coefficient [m^{-1}]
τ_d	optical thickness of one particle bed depth, κd_p
ω	scattering albedo, σ_s/κ.

Superscripts

d	dispersion
s	stagnant parameter.

Subscripts

B	bulk of packed medium
c	convection
e	effective parameter
f	fluid phase
h	higher value
p	particle phase
r	radiation
w	heat transfer wall
∞	parameter far from the heat transfer plate (bulk of the bed).

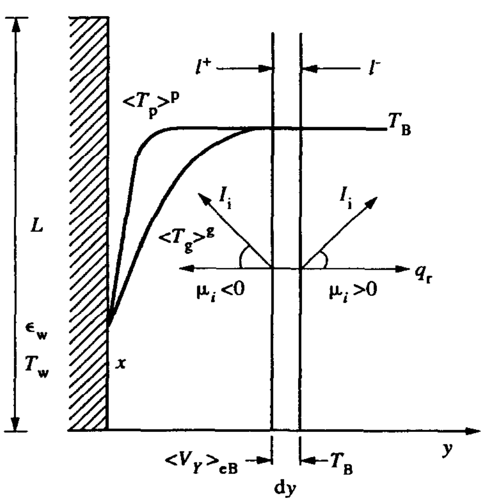

FIG. 1. Coordinates and boundary conditions.

(i) The bed consists of large (geometric range) opaque spheres and the particle surfaces and heat transfer plates are gray ones, so the radiation properties do not change with wavelengths.

(ii) The fluid flowing through the bed is considered to be transparent to radiation.

(iii) The porosity changes only in the transverse direction y.

General equations

Under previous assumptions, the boundary layer equations describing the combined convective and radiative heat transfer in packed beds may be written as:

Momentum equation,

$$-\frac{\partial}{\partial X}\langle p\rangle^f + \frac{\mu_f}{\delta}\frac{\partial^2\langle u\rangle}{\partial y^2} - \frac{\mu_f\langle u\rangle}{K} - \rho_f C\langle u\rangle^2 = 0, \tag{1}$$

where $\langle u \rangle$ is the volume-average velocity parallel to the wall (X direction).

Energy equation,

$$(\rho C_p)_f \langle u \rangle \frac{\partial \langle T \rangle}{\partial x} = \frac{\partial}{\partial y}\left(k_e \frac{\partial \langle T \rangle}{\partial y}\right) - \frac{\partial}{\partial y}\langle q_r \rangle. \quad (2)$$

Equation for radiative flux,

$$\frac{\partial}{\partial x}\langle q_r \rangle = 4a\sigma \langle T \rangle^4 - a \int_{4\pi} \langle i(x,\mu) \rangle \, d\omega. \quad (3)$$

Transfer equation for azimuthally symmetric radiation in one-dimension case,

$$\mu \frac{\partial \langle i(x,\mu) \rangle}{\partial x} = -(\sigma_s + a)\langle i(x,\mu) \rangle + \frac{1}{\pi} a\sigma \langle T \rangle^4 + \frac{\sigma_s}{2}\int_{-1}^{1} \langle i(x,\mu') \rangle P(\mu,\mu') \, d\mu' \quad (4)$$

where μ is the directional cosine with respect to coordinate y ($\mu = \cos\theta$) and P is the scattering phase function.

These equations are in the volume average form (notation $\langle\ \rangle$) obtained from averaging the microscopic conservation equations over a representative volume including both the fluid and the solid phase [17].

The volume-average quantity of W associated with one phase i is defined as:

$$\langle W \rangle = \frac{1}{v}\int_{V_i} W_i \, dV = \frac{V_i}{V}\frac{1}{V_i}\int_{V_i} W \, dV = \beta \langle W \rangle^i \quad (5)$$

with $\beta = \delta$ if $i = g$ and $\beta = 1-\delta$ if $i = p$ where δ is the local porosity.

These equations are combined with empirical relations for the permeability, inertial coefficient, equivalent molecular and dispersion diffusivity [8, 18, 19]. Here it is assumed that the local thermal equilibrium exists between the solid phase and the fluid phase, which means that the local temperature difference between the phases ($T_s - T_f$) is small or the local temperature gradients ∇T_s and ∇T_f are almost equal [8]. The validity of this assumption is checked to be true for the present cases with the heterogeneous energy equations.

The parameters

The term $\langle p \rangle^f$ in equation (1) is the intrinsic fluid phase average pressure since the pressure read on a pressure gauge actually represents the average pressure inside the fluid phase [2]. K and C are the permeability and inertia coefficients, which, for the packed bed of spheres are [20]:

$$K = \frac{d_p^2 \delta^3}{150(1-\delta)^2} \quad (6)$$

$$C = \frac{1.75(1-\delta)}{d_p \delta^3}. \quad (7)$$

The porosity, δ, is assumed to vary exponentially with the distance from the plate [1]:

$$\delta = \delta_\infty [1 + D\exp(-D^* y/d_p)]. \quad (8)$$

δ_∞ in above equations is the bed porosity far from the wall, the constants D and D^* are experimental parameters and taken as $D^* = -6$ and $D = (1-\delta_\infty)/\delta_\infty$ [9].

The effective conductivity k_e in equation (2) includes the stagnant thermal conductivity k_e^s and the dispersion effect k_e^d, the former is calculated with the formulae of Zehner and Schlunder [21],

$$\frac{k_e^s}{k_f} = 1 - (1-\delta)^{1/2} + (1-\delta)^{1/2}\frac{2}{(1-B/R_k)} \times \left[\frac{(1-B)/R_k}{(1-B/R_k)^2}\ln\frac{R_k}{B} - \frac{B+1}{2} - \frac{B-1}{1-B/R_k}\right] \quad (9)$$

where R_k is the ratio of the thermal conductivities of the particle and the fluid phase, and $B = 1.25[(1-\delta)/\delta]^{10/9}$ for a packed bed of spheres.

The dispersion conductivity k_e^d is calculated from the empirical formula given by Hunt and Tien [9],

$$k_e^d = \gamma (\rho C_p)_f u d_p l \quad (10)$$

where $\gamma = 0.1$ and $l = y/d_p$ when $y \leqslant d_p$ and $l = 1.0$ when $y > d_p$.

The scattering phase function in equation (4) is related to single-particle scattering function,

$$P(\mu,\mu') = \frac{1}{\pi}\int_0^\pi P[\theta(\mu',\phi' = 0 \to \mu,\phi)] \, d\phi \quad (11)$$

where

$$\cos\theta = \mu\mu' + (1-\mu'^2)^{1/2}\cos\phi \quad (12)$$

and

$$P(\theta) = \frac{8}{3\pi}(\sin\theta - \theta\cos\theta). \quad (13)$$

Numerical formulation of the radiation problem

The discrete-ordinate method is used to approximate the governing differential–integral equations into differential forms. It is based on the division of the azimuthally symmetric radiation flux into N discrete conical streams, $I(x,\mu_i)$, $i = 1$–N [22]. So equations (3) and (4) are replaced by a discrete set of equations for a finite number of ordinate directions,

$$\mu_i \frac{d\langle i(x,\mu_i) \rangle}{dx} = -(\sigma_s + a)\langle i(x,\mu_i) \rangle + \frac{a}{\pi}\sigma \langle T \rangle^4 + \frac{\sigma_s}{2}\sum_{j=1}^{N} w_j \langle i(x,\mu_j) \rangle P(\mu_i,\mu_j) \quad (14)$$

$$\frac{d}{dx}\langle q_r \rangle = 4a\sigma \langle T \rangle^4 - 2\pi a \sum_{j=1}^{N} \langle i(x,\mu_j) \rangle w_j. \quad (15)$$

The divisions u_i correspond to the zeros of the Legendre polynomials $L_N(\mu)$ and the weights w_j are given by

$$w_i = \frac{1}{L'_N(\mu_i)} \int_{-1}^{1} \frac{\mu}{\mu-\mu_i} \, d\mu. \quad (16)$$

In order to solve the above equations, the radiative properties of the particulate must be defined as a function of the absorption and the diffusion characteristics of the individual particles. For low porosity systems like packed or fluidized beds, whether the scattering is dependent or independent is an up-to-date scientific subject. Brewster and Tien [23] concluded that the independent scattering assumption is valid in packed beds of large particles even for a close packed arrangement. They proposed the limit of $c/\lambda < 0.3$ (i.e. $\delta > 0.3$), where c is the average interparticle distance and λ the wavelength of radiation. On the contrary, Singh and Kaviany's recent investigation [24] based on Monte-Carlo simulation of the radiation showed that the deviation from the independent theory may be significant even for high porosity particulate ($\delta_e = 0.935$) and increases with a decrease in porosity. They also showed [25] that the dependent properties for a bed of opaque spheres can be obtained from their independent properties by scaling the optical thickness while leaving the albedo and the phase function unchanged and the scaling factor was presented as the following form,

$$S_r = 1.0 + 1.84(1-\delta) - 3.15(1-\delta)^2 + 7.20(1-\delta)^3 \quad \text{for } \delta > 0.3. \quad (17)$$

Thus the scattering and absorption coefficients can be expressed as [24, 26]

$$\sigma_s = 1.5(1-\varepsilon)(1-\delta)S_r/d_p \quad (18)$$

$$a = 1.5\varepsilon(1-\delta)S_r/d_p \quad (19)$$

where ε is the particle emissivity. Thus the extinction coefficient $\kappa = a + \sigma_s$ is only related to the porosity of the bed and the size of the particles.

Non-dimensional formulation of the problem

When introducing the non-dimensional variables, $X = x/d_p$, $Y = y/d_p$, $U = \langle u \rangle / u_\infty$, $I = \langle i \rangle / \sigma T_h^4$, $\theta = \langle T \rangle / T_h$, the governing equations (1)–(4) can be transformed into non-dimensional form,

$$\frac{\mu_f}{\mu_{f\infty}} \frac{K_\infty}{K} U + \frac{\rho_f}{\rho_{f\infty}} \frac{C}{C_\infty} Re_c U^2 - 1 - Re_c - \frac{\mu_f}{\mu_{f\infty}} \frac{Da}{\delta} \frac{d^2 U}{dY^2} = 0 \quad (20)$$

$$Bo \frac{(\rho C_p)_f}{(\rho C_p)_{f\infty}} U \frac{\partial \theta}{\partial X} = \frac{4N}{\tau_d} \frac{\partial}{\partial Y}\left(\frac{k_e}{k^s_{e\infty}} \frac{d\theta}{dY}\right) - 4\tau_d R_K (1-\omega)\left[\theta^4 - \frac{\pi}{2} \sum_{j=1}^{N} I_j w_j\right] \quad (21)$$

$$\mu_i \frac{1}{\tau_d R_k} \frac{\partial I_i}{\partial Y} = -I_i + \frac{(1-\omega)}{\pi} \sigma\theta^4 + \frac{\omega}{2} \sum_{j=1}^{n} w_j I_j P_{i,j} \quad (22)$$

where

$$Da = K_\infty/d_p^2, \quad Re_c = K_\infty C_\infty u_\infty/\nu_{f\infty},$$

$$Bo = (\rho C_p)_{f\infty} u_\infty/\sigma T_h^3, \quad N = k^s_{e\infty}\kappa_\infty/4\sigma T_h^3 d_p,$$

$$R_k = \kappa/\kappa_\infty, \quad \alpha^s = k_e^s/(\rho C_p)_f, \quad \kappa = a + \sigma_s,$$

$$T_h = \max(T_B, T_w), \quad \tau_d = \kappa_\infty d_p.$$

Equation (19) is obtained from (1) accounting for the expression of the pressure gradient $(\partial/\partial x)\langle p \rangle^f$ on the basis of Ergun's equation [20]:

$$\frac{\partial}{\partial x}\langle p \rangle^f = -\frac{\mu_f u_\infty}{K_\infty} - \rho_f C_\infty u_\infty^2. \quad (23)$$

In the above equations the local temperature is used as the reference temperature to determine the thermal physical parameters. But in order to focus our attention on the interaction between different heat transfer modes, the influence of the dependence of temperature on thermal physical parameters is neglected in this paper, i.e. the ratio of $\rho_f/\rho_{f\infty}$, $\mu_f/\mu_{f\infty}$ and $(\rho C_p)_f/(\rho C_p)_{f\infty}$ are taken as unity.

The dimensionless Boltzmann number $Bo = (\rho C_p)_f u_\infty / \sigma T_h^3$ indicates the relative importance of convective and radiative heat transfer. In the early researches on interaction of radiation with other heat transfer modes the main attention was paid to the interaction between conductive and radiative heat transfer and a conduction–radiation parameter (Planck number) $N = k_e^s \kappa / 4\sigma T_h^3$ was introduced. The two dimensionless parameters Bo and N are related through Peclet number,

$$Bo = 4NPe/\tau_d \quad (24)$$

where $Pe = u_\infty d_p \alpha^s_\infty$.

The dimensionless boundary conditions are,

$$Y = 0, \quad U = 0, \quad \theta_w = T_w/T_h \quad (25)$$

$$I_i = \varepsilon_w \theta^4/\pi + 2(1-\varepsilon_w) \sum_{j=1}^{N/2} I_j w_j |\mu_j| \quad (i = N/2+1, N) \quad (26)$$

$$Y \to \infty, \quad U = 1, \quad \theta_B = T_B/T_h \quad (27)$$

$$\partial I_i/\partial Y = 0 \quad (i = N/2+1, N) \quad (28)$$

$$I_i = I_{N/2+1} \quad (i = 1, N/2). \quad (29)$$

The conductive–convective and radiative heat transfer Nusselt number can be expressed as,

$$Nu_c = \frac{h_c d_p}{k^s_{e\infty}} = \frac{k_e}{k^s_{e\infty}} \frac{1}{\theta_B - \theta_w} \left.\frac{\partial \theta}{\partial Y}\right|_{Y=0} \quad (30)$$

$$Nu_r = \frac{h_r d_p}{k^s_{e\infty}} = \frac{Pe}{Bo(\theta_w - \theta_B)}\left(\varepsilon_w \theta_w^4 - 2\pi\varepsilon_w \sum_{j=1}^{N/2} I_j w_j |m_j|\right). \quad (31)$$

But in most of the previous investigations the longitudinal coordinate x was often used as length dimension in Nusselt number and Peclet number, the relation between the two forms of Nusselt number is:

$$Nu_{ix} = \frac{h_i x}{k^s_{e\infty}} = Nu_i \left[\frac{x}{Pe}\right]^{1/2} Pe_x^{1/2} \qquad (32)$$

where subscript i represents c and r respectively, for the conduction–convection and radiative components and $Pe_x = ux/\alpha^s$.

Numerical procedure

Numerical solutions of equations (20)–(22) with the boundary conditions (25)–(29) have been obtained with the finite differential method. A finer grid is used near the heat transfer surface and upwind region to account for the steep velocity and temperature gradients. The center differencing is used for the spatial derivatives except for the convective terms for which upwind differencing is used along with the linearization of the momentum and energy equations. The calculation is iterated until the solution converges and the accuracy of the finite difference solution is tested by increasing the number of grid points and comparing the results in the case where Darcy's law is used and no radiation occurs with the well-known formula of Cheng [27],

$$Nu_x = 0.564\, Pe_x^{1/2}. \qquad (33)$$

RESULTS AND DISCUSSION

In order to investigate the relative importance of the convective and radiative transfer and the interaction of the two transfer modes, the prediction is carried out including the non-Darcian effects. The effects of controlling parameters and of the direction of heat flux are also checked, whose variation ranges are shown in Table 1.

Non-Darcian effects

When only Darcy's law is used for the forced convection in packed beds, it means that the transverse distribution of the fluid velocity and of the porosity are uniform and no dispersion appears, so the momentum equation (20) reduces to $U = 1$. Whereas if the boundary effect is considered, the fluid velocity at the solid boundary decreases to zero because of the shear force. The larger porosity near the wall causes channelling flow as well as the variation of the thermal diffusion in this region. The inertia effect increases the pressure drop across the bed for large flow rates. For a given particle Reynolds number, this phenomenon retards the extent of channelling when the variable porosity is considered. Thus the boundary and inertia effects reduce the heat transfer and the channelling effect enhances the heat transfer. The radial thermal dispersion also strengthens convection. These general trends of influence of non-Darcian effects were obtained in recent years [9].

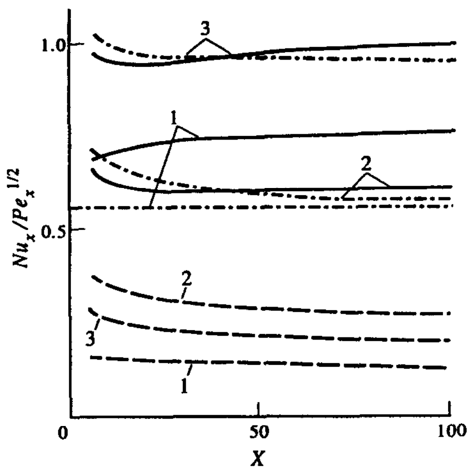

FIG. 2. Predicted results with different approximations $Re = 100$, $Bo = 10$, $T_w/T_B = 0.5$, $\varepsilon_w = \omega = 0.5$. —— Nu_{cx}; —·— Nu_{cx}, no radiation; – – –Nu_{rx}. 1. Darcy's law; 2. non-Darcian flow, no dispersion; 3. dispersion considered.

The relative importance of radiation and the effect on the convection of these different approximations are shown in Fig. 2. It can be seen that the non-Darcian effects enhance the convective transfer, especially when the dispersion diffusion is accounted for in the region of leading edge when no radiation appears. When the radiative transfer becomes non-negligible, the convective transfer rate varies because of the changes of the temperature distribution (Fig. 3). For the case illustrated in Fig. 2, the convection decreases at the leading edge and increases in the down-stream regime when the non-Darcian effects are considered and the radiation enhances convection all along the plate if Darcy's law is used. This decrease or increase means that the heat absorbed by the particles near the wall from the bed bulk by radiation is smaller or larger than that emitted to the wall, so the temperature difference between the wall and the bed adjacent to it decreases or increases.

Table 1. Variation ranges of controlling parameters

Bo	N	Re	T_w/T_B	ε_w	ω	R_k	δ	Pr_f
1, 10	0.05	10, 10^2	0.1, 0.5	0.0, 0.5	0.0, 0.5	10	0.4	0.7
20	0.005	10^3	0.9	1.0	1.0			

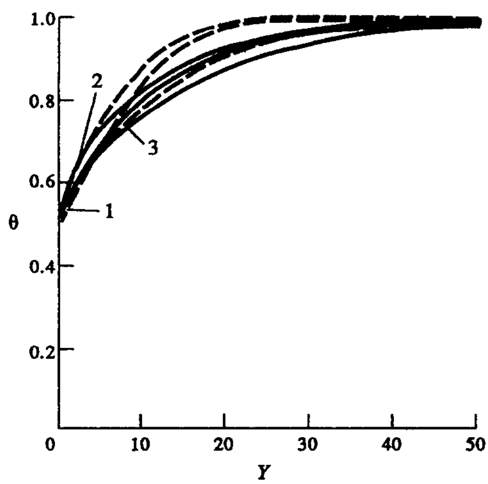

FIG. 3. Temperature profiles with different approximations calculating conditions are same with Fig. 2. —— conduction+convection+radiation; – – – conduction+convection.

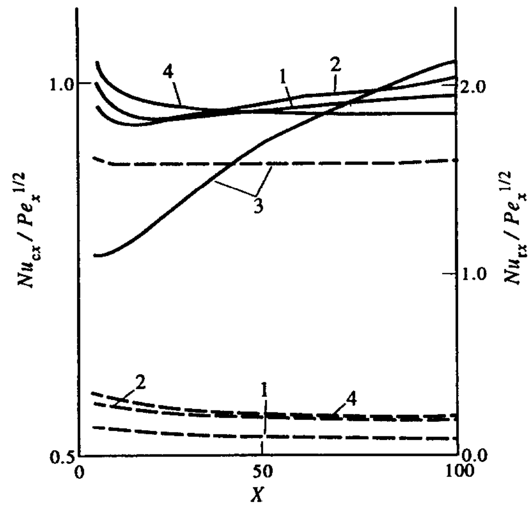

FIG. 4. Influence of Boltzmann number $Re = 100$, $T_w/T_B = 0.5$, $\varepsilon_w = \omega = 0.5$. —— Nu_{cx}; – – – $Nu_r x$. 1. $Bo = 20$; 2. $Bo = 10$; 3. $Bo = 1$; 4. $Bo = 10$, no interaction.

The absolute values and relative importance of the radiative transfer change with the different approximations used. When the influence of the solid boundary, inertia and channelling effects, which are limited to the region just near the wall, are considered, the radiation is enhanced. This indicates that the channelling effect is dominant for the considered situations since the solid boundary and inertia effects weaken the convective transfer and increase the boundary thickness. The dispersive mixing strengthens the convection obviously and induces the temperature field to be sharper near the wall but to present a deeper heat penetrating depth (Fig. 3). Thus when the dispersion effect is included, the radiation contribution decreases in comparison with the situations where only the solid boundary, inertia and channelling effects are accounted for. In addition, Fig. 3 proves that the thickness of heat transfer boundary increases when radiation occurred.

Influence of Boltzmann number, Bo

For the forced convection in packed beds at high temperature, all of the three heat transfer modes, conduction, convection and radiation are significant, their relative influences are governed by controlling dimensionless parameters *Pe*, *Bo* or *N*, T_w/T_B or T_B/T_w, ε_w, ω, and so on.

The parameter $Bo = (\rho C_p)_f u/\sigma T_h^3$ indicates the relative importance of convective and radiative transfer, its influence is shown in Fig. 4. When Peclet number remains constant, the change of Boltzmann number means the change of Planck number according to equation (24). It can be found that the radiative transfer rate increases very fast as the parameter *Bo* decreases. For the parameters shown in the figure, the ratio of radiation with respect to convection is about 10% for $Bo = 20$ and about 20% when $Bo = 10$, whereas the radiative transfer is the dominant mode of heat exchange when $Bo = 1.0$. In agreement with the previous analysis, the convection would be weakened by the radiation at the leading edge but enforced in downstream region. The extent of interaction of the two heat transfer modes on radiation can also be found in Fig. 4, in which the curve 4 is related to radiative Nusselt number based on the temperature distribution when the interaction is omitted. For the situation considered, the interaction would decrease the radiative transfer rate because of the deeper heat penetration when the two transfer modes act together.

Influence of particle Reynolds number

The influence of particle Reynolds number, i.e. the Peclet number when the ratio of conductivities of solid and fluid does not change, should be checked in two ways: *Bo* or *N* remains constant as shown in Figs. 5 and 6, respectively. In these figures, the logarithmic scale is used for longitudinal coordinates since the local Peclet number changes with particle Reynolds number. The constant Boltzman number means that radiation follows the change of convection. So it can be seen from Figs. 5(a) and (b), where $Bo = 10$ and 1, respectively, that the radiative Nusselt number and the Reynolds number vary with the same trend. When $Bo = 10$, convection is the dominant mode for all the investigated range of Reynolds number whereas the radiation is the dominant mode for $Re \geqslant 10^2$ when $Bo = 1$. Figure 5(c) shows that the occurrence of radiation strengthens slightly the convection for small Reynolds number and weakens the convection for large Reynolds number under the other control parameters given in the figure. In addition a constant Planck number means that the ratio of conductive and

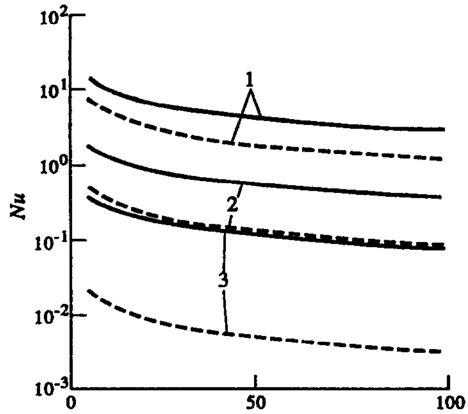

(a)

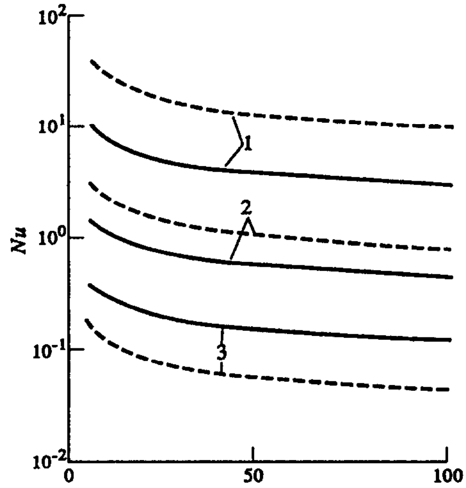

(b)

FIG. 5. (a) Influence of Reynolds number with $Bo = 10$. $T_w/T_B = 0.5$, $\varepsilon_w = \omega = 0.5$. —— Nu_c; --- Nu_r. 1. $Re = 10^3$; 2. $Re = 10^2$; 3. $Re = 10$. (b) Influence of Reynolds number with $Bo = 1$. $T_w/T_B = 0.5$, $\varepsilon_w = \omega = 0.5$. —— Nu_c; --- Nu_r. 1. $Re = 10^3$; 2. $Re = 10^2$; 3. $Re = 10$.

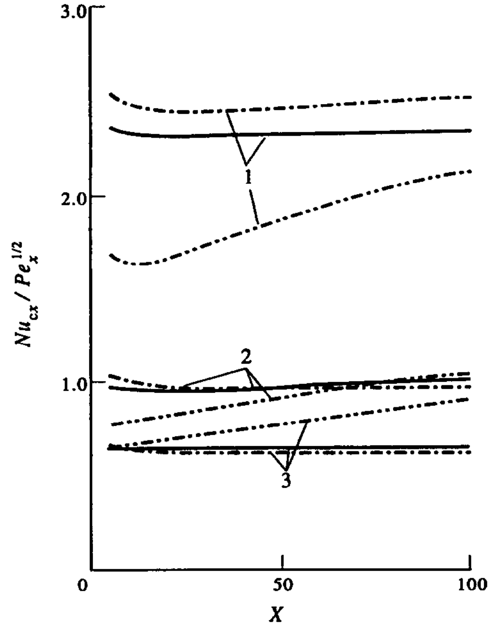

(c)

FIG. 5(c). Influence of radiation on convection with Bo as parameter. $T_w/T_B = 0.5, \varepsilon_w = \omega = 0.5$. —— $Bo = 10$; —··— $Bo = 1$; —·— no radiation. 1. $Re = 10^3$; 2. $Re = 10^2$; 3. $Re = 10$.

radiative transfers does not change as the Reynolds number changes. It appears in Figs. 6(a) and (b), where $N = 0.05$ and 0.005, respectively, that the variation of radiative Nusselt number with the increase of Reynolds number is smaller than at constant Boltzmann number (Figs. 5(a) and (b)), especially for the cases $N = 0.005$. Radiation is the dominant heat transfer mode for $Re \leqslant 10^2$ when $N = 0.05$ and for all considered range of Reynolds number when $N = 0.005$. The effect of radiation on convection shown in Fig. 6(c) is similar with the cases at constant Boltzmann number. It is interesting to notice that convection is affected by radiation very strongly for small Reynolds numbers, especially in the downstream regime.

Influence of relative temperature, T_w/T_B

When the particle Reynolds number Re and the convection–radiation parameter Bo remain constant if the relative temperature T_w/T_B changes from 0.1 to 0.9, the radiative transfer rate increases obviously (Fig. 7), especially in the downstream region. The ratio of radiative Nusselt numbers when the relative temperature T_w/T_B is 0.9 and 0.1, respectively, $Nu_{r,0.9}/Nu_{r,0.1}$, equals 60.5 at the position $X = x/d_p = 100$. The effect of radiation on convective transfer varies as a function of the relative temperature T_w/T_B. For $T_w/T_B = 0.1$, the radiation always enhances the convection, but for $T_w/T_B = 0.9$, the radiation reduces the convective transfer in the considered longitudinal range. The increase or decrease of the convection by radiation just depends on the sign of the net radiation absorbed by the particles. It must be pointed out that this conclusion can be discussed because the model assumption of independence of thermophysical properties on temperature is not respected when the temperature difference between the plate and the bed is large and its influence on heat transfer in packed beds will be investigated in a later work.

Effects of wall emissivity and scattering albedo of the bed

When the emissivity of the heat transfer plate equals unity, it would absorb all radiative energy emitted by the bed medium, so the radiative Nusselt number is maximum and its value is roughly equal to the convective component when the other parameters remain

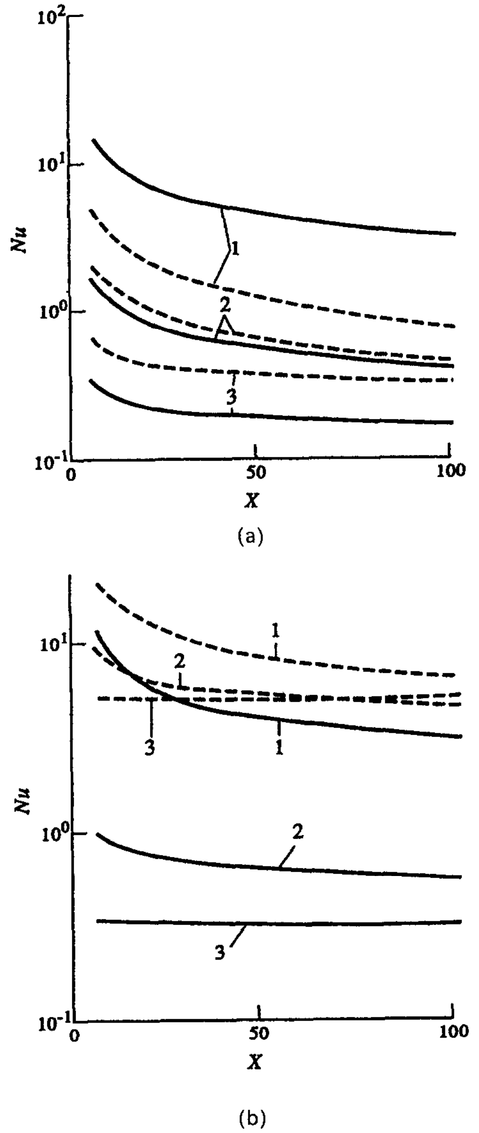

FIG. 6. (a) Influence of Reynolds number with $N = 0.05$. $T_w/T_B = 0.5$, $\varepsilon_w = \omega = 0.5$. —— Nu_c; - - - Nu_r. 1. $Re = 10^3$; 2. $Re = 10^2$; 3. $Re = 10$. (b) Influence of Reynolds number with $N = 0.005$. $T_w/T_B = 0.5$, $\varepsilon_w = \omega = 0.5$. —— Nu_c; - - - Nu_r. 1. $Re = 10^3$; 2. $Re = 10^2$; 3. $Re = 10$.

constants (as shown in Fig. 8). In addition when ε_w becomes zero, the radiative transfer between the solid boundary and the packed bed vanishes. But in this case the convection is obviously strengthened because the bed medium absorbs the heat by radiation from the bed bulk, on the other hand, it is evidently reduced when $\varepsilon_w = 1.0$.

The bed medium will not take part in the radiative transfer when the scattering albedo becomes unit, it means that particles scatter all radiant energy reaching them. For this situation the radiative transfer coefficients would be zero when the bed medium is considered as semi-infinite and the convective transfer

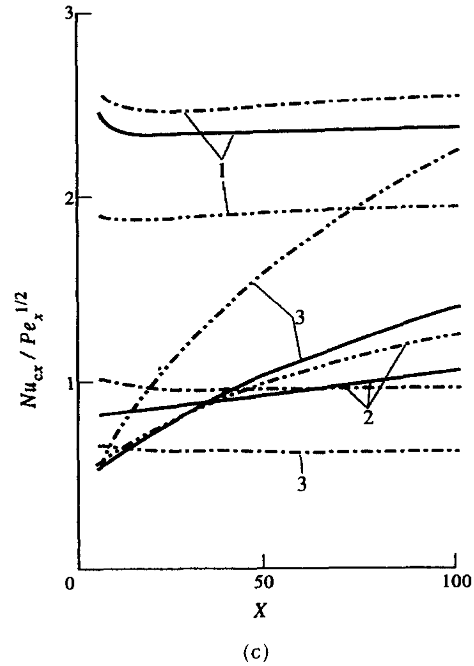

FIG. 6(c). Influence of radiation on convection with N as parameter. $T_w/T_B = 0.5$, $\varepsilon_w = \omega = 0.5$. —— $N = 0.05$; —‥— $N = 0.005$; —·— no radiation. 1. $Re = 10^3$; 2. $Re = 10^2$; 3. $Re = 10$.

rate would remain the same as there is no radiation. When the scattering albedo changes from 0.5 to zero, the radiative component changes only slightly, but the convective transfer is enhanced significantly.

Effects of the direction of heat flux

All the above predicted results are obtained in the cases of $T_B > T_w$, i.e. the heat is transferred from the

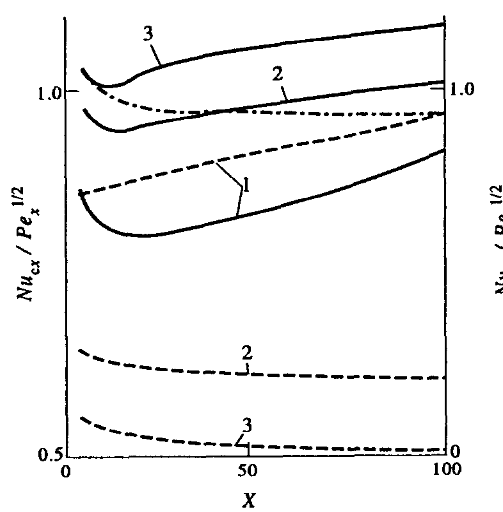

FIG. 7. Influence of relative temperature. $Re = 100$, $Bo = 10$, $\varepsilon_w = \omega = 0.5$. —— Nu_{cx}; —·— Nu_{xx}, no radiation; - - - Nu_{rx}. 1. $T_w/T_B = 0.9$; 2. $T_w/T_B = 0.5$; 3. $T_w/T_B = 0.1$.

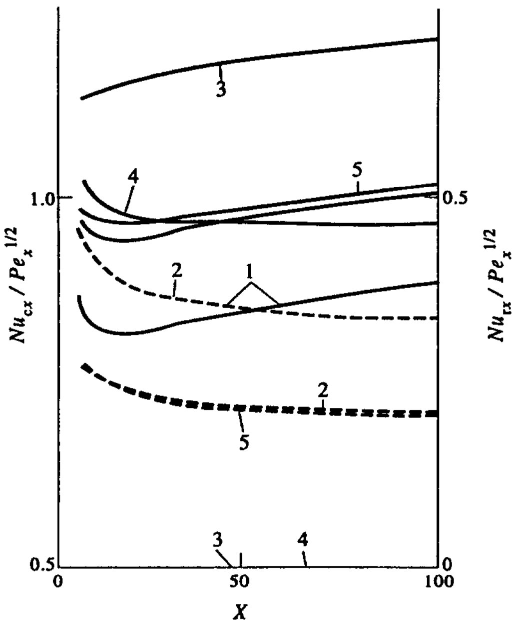

FIG. 8. Influence of plate emissivity and scattering albedo of packed bed. $Re = 100$, $Bo = 10$, $T_w/T_B = 0.5$. —— Nu_{cx}; --- Nu_{rx}. 1. $\varepsilon_w = 1.0$, $\omega = 0.5$; 2. $\varepsilon_w = 0.5$, $\omega = 0.5$; 3. $\varepsilon_w = 0.0$, $\omega = 0.5$; 4. $\varepsilon_w = 0.5$, $\omega = 1.0$; 5. $\varepsilon_w = 0.5$, $\omega = 0.0$.

bed to the plate. When only the convection mode occurs and the thermal properties remain constant, the convective Nusselt number does not change with the direction of heat flux. But as the radiative transfer becomes important, both the convective and radiative transfer components would change with the direction of heat flux. Comparing the predicted results when

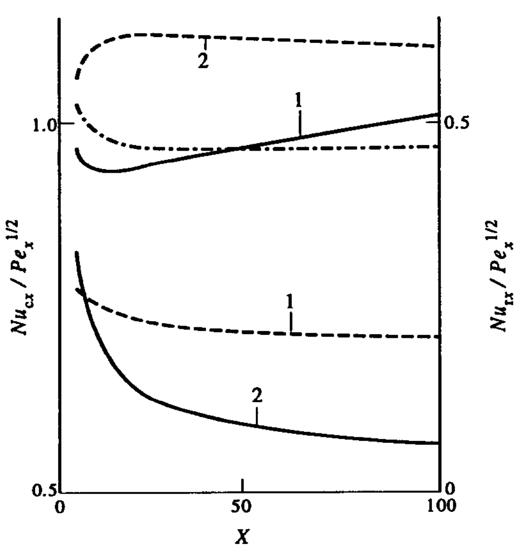

FIG. 9. Influence of direction of heat flux. $Re = 100$, $Bo = 10$, $\varepsilon_w = \omega = 0.5$. —— Nu_{cx}; —·— Nu_{cx}, no radiation; --- Nu_{rx}. 1. $\theta_B = 1.0$, $\theta_w = 0.5$; 2. $\theta_B = 0.5$, $\theta_w = 1.0$.

the direction of heat flux changed, just as shown in Fig. 9, it can be found in general that the radiative transfer rates would be larger when the heat flux is from the heat transfer plate into the bed than when the heat flux is in the opposite direction. It is also shown that convection is generally reduced by radiation when $T_w > T_B$, except when the emissivity of the heat transfer surface is small, in this latter case the bed medium emits heat energy transferred by convection to the bed bulk and therefore enhances the convective transfer.

CONCLUSION

This paper presents numerical predictions of forced convection and radiation heat transfer between a flat plate and the packed medium at high temperature. It is shown that the radiative transfer rate and the interaction of different heat transfer modes are dependent on the different approximations made for hydrodynamics and heat transfer in packed beds and the direction of heat flux. Generally, the radiative transfer rate increases with the decrease of: convection–radiation parameter, conduction–radiation parameter, plate and bed temperatures, scattering albedo of bed medium; and the increase of: Reynolds number, wall emissivity. The convection is enhanced when the heat flux direction is from the bed to the plate and is reduced when the heat flux is in the opposite direction (in the cases considered in this paper). When the emissivity of the plate is small, the convection would always be enhanced by radiation regardless of the heat flux direction. It should be indicated that the results obtained in this paper illustrate the main tendencies due to radiation effects since more theoretical and experimental studies are needed in packed beds to understand the hydrodynamic and heat transfer mechanisms more clearly and the choice of some empiric formulas, such as porosity distribution and dispersion, more reasonable.

REFERENCES

1. B. C. Chandrasekhara and D. Vortmeyer, Flow model for velocity distribution in fixed porous beds under isothermal conditions, *Fluid Dyn.* **12**, 105–111 (1979).
2. K. Vafai and C. L. Tien, Boundary and inertia effects on flow and heat transfer in porous media, *Int. J. Heat Mass Transfer* **24**, 195–203 (1981).
3. K. Vafai and C. L. Tien, Boundary and inertia effects on convective mass transfer in porous media, *Int. J. Heat Mass Transfer* **25**, 1183–1190 (1982).
4. K. Vafai, Convective flow and heat transfer in variable-porosity media, *J. Fluid Mech.* **147**, 223–259 (1984).
5. O. A. Plumb, The effect of thermal dispersion on heat transfer in packed bed boundary layers, *ASME–JSME Joint Thermal Conf. Proc.*, Vol. 2, pp. 17–21 (1983).
6. S. Whitaker, Local thermal equilibrium: an application to packed bed catalytic reactor design, *Chem. Engng Sci.* **41**, 2029–2039 (1986).
7. P. Cheng and D. Vortmeyer, Transverse thermal dis-

persion and wall channelling in a packed bed with forced convection flow, *Chem. Engng Sci.* **4,** 2523–2532 (1988).
8. C. L. Tien and M. L. Hunt, Boundary-layer flow and heat transfer in porous beds, *Chem. Engng Process.* **21,** 53–63 (1987).
9. M. L. Hunt and C. L. Tien, Non-Darcian convection in cylindrical packed beds, *ASME J. Heat Transfer* **110,** 378–384 (1988).
10. T. Tsostas and E.-U. Schlunder, Heat transfer in packed beds with fluid flow: remarks on the meaning and the calculation of a heat transfer coefficient at the wall, *Chem. Engng Sci.* **45,** 819–937 (1990).
11. F. C. Chou, W. Lien and S. H. Lin, Analysis and experiment of non-Darcian convection in horizontal square packed-sphere channels—I. Forced convection, *Int. J. Heat Mass Transfer* **35,** 195–205 (1992).
12. C. L. Tien, Thermal radiation in packed and fluidized beds, *ASME J. Heat Transfer* **110,** 1230–1242 (1988).
13. J. A. Harris and T. G. Lenz, Experimental heat transfer in a packed bed in which radiation, conduction and convection are all significant, *ASME HTD* **46,** 49–59 (1985).
14. C. Bouallou and J. F. Sacadura, Thermal radiation, convection and conduction in porous media contained in two-dimensional vertical cavities, *ASME J. Heat Transfer* **113,** 255–258 (1991).
15. H. Yoshida, J. H. Yun and R. Echigo, Transient characteristics of combined conduction, convection and radiation heat transfer in porous media, *Int. J. Heat Mass Transfer* **33,** 847–857 (1990).
16. G. Flamant, J. D. Lu and B. Variot, Towards a generalized model for vertical walls to gas–solid fluidized beds heat transfer, Part 2. Radiation transfer and temperature effects, *Chem. Engng Sci.* **48**(3), 2493–2503 (1993).
17. S. Whitaker, Advances in theory of fluid motion in porous media, *A.I.Ch.E. Jl* **13,** 420–427 (1969).
18. C. T. Hsu and P. Cheng, Thermal dispersion in a porous medium, *Int. J. Heat Mass Transfer* **33,** 1587–1597 (1990).
19. J. D. Lu, G. Flamant and P. Snabre, Towards a generalized model for vertical walls to gas–solid fluidized beds heat transfer, Part 1. Particle convection and gas convection, *Chem. Engng Sci.* **48**(3), 2479–2492 (1992).
20. S. Ergun, Fluid flow through packed columns, *Chem. Engng Pregr.* **48,** 89–94 (1952).
21. P. Zehner and E. U. Schlunder, Wärmeleitfähigkeit von schüttungen bei massigen temperaturen, *Chem. Ing. Tech.* **42,** 933–941 (1970).
22. S. Chandrasekhar, *Radiative Transfer*. Dover, New York (1960).
23. M. Q. Brewster and C. L. Tien, Radiative transfer in packed fluidized-beds: dependent versus independent scattering, *ASME J. Heat Transfer* **104,** 573–579 (1982).
24. B. P. Singh and M. Kaviany, Independent theory versus direct simulation of radiation heat transfer in packed beds, *Int. J. Heat Mass Transfer* **34,** 2869–2882 (1991).
25. B. P. Singh and M. Kaviany, Modelling radiative heat transfer in packed beds, *Int. J. Heat Mass Transfer* **35,** 1397–1405 (1992).
26. R. Siegel and R. J. Howell, *Thermal Radiation Transfer* (2nd Edn). Hemisphere, New York (1981).
27. P. Cheng, Combined free and forced convection flow about inclined surfaces in porous media, *Int. J. Heat Mass Transfer* **20,** 807–814 (1977).